0026-895X/97/050839-07$3.00/0

MOLECULAR PHARMACOLOGY, **52:**839–845 (1997).

Mitindomide Is a Catalytic Inhibitor of DNA Topoisomerase II That Acts at the Bisdioxopiperazine Binding Site

BRIAN B. HASINOFF, ANDREW M. CREIGHTON, HANNA KOZLOWSKA, PADMAKUMARI THAMPATTY, WILLIAM P. ALLAN, and JACK C. YALOWICH

Faculty of Pharmacy, University of Manitoba, Winnipeg, Manitoba, R3T 2N2 Canada (B.B.H., H.K.), Department of Pharmacology, University of Pittsburgh School of Medicine and Cancer Institute, Pittsburgh, Pennsylvania 15261(P.T., W.P.A., J.C.Y.), and Medicinal Chemistry Laboratory, Department of Reproductive Physiology, St. Bartholomew's Hospital Medical College, West Smithfield, London, United Kingdom (A.M.C.)

Received March 17, 1997; Accepted July 31, 1997

SUMMARY

The antitumor drug mitindomide (NSC 284356) was shown to inhibit the decatenation activity of human and Chinese hamster ovary (CHO) topoisomerase II [DNA topoisomerase (ATP-hydrolyzing), EC 5.99.1.1]. Mitindomide did not induce the formation of topoisomerase II-DNA covalent cleavable complexes in CHO cells. These results taken together indicate that mitindomide is a catalytic/noncleavable complex-forming-type inhibitor of topoisomerase II. The growth inhibitory effects of mitindomide and dexrazoxane toward a sensitive parent CHO cell line and the dexrazoxane-resistant DZR cell line, which is highly (500-fold) resistant to the bisdioxopiperazine dexrazoxane, were measured. The DZR cell line was shown to be 30-fold cross-resistant to mitindomide. Mitindomide, like dexrazoxane, was shown to inhibit cleavable complex formation by the topoisomerase II poison etoposide. The attenuated inhibition of etoposide-induced cleavable complexes in DZR compared with CHO cells was, likewise, very similar for dexrazoxane and mitindomide. Together these results suggest that mitindomide acts at the same site on topoisomerase II as does dexrazoxane and other bisdioxopiperazines. Various molecular parameters obtained by molecular modeling were compared for mitindomide and dexrazoxane. Mitindomide, which is conformationally very rigid, has highly coplanar imide rings, as does dexrazoxane in the solid state. Other molecular parameters, such as the imide nitrogen-to-imide nitrogen bond distances, and polar and nonpolar surface areas were also very similar. Thus, it is concluded that mitindomide exerts its antitumor effects through its inhibition of topoisomerase II by binding to the bisdioxopiperazine binding site.

Mitindomide (NSC 284356) (Fig. 1) and a number of its analogs have been shown to have good antitumor activity (1–3). Even though mitindomide has been shown to slowly (over 12 hr) promote DNA-interstrand cross-linking (4), the mechanism by which mitindomide or its analogs exert their antitumor effects has never been identified. Problems with low aqueous solubility of mitindomide (3, 5, 6) led to the development of a number of more soluble *N*-substituted analogs (3, 4, 7–9), some of which also displayed good antitumor activity. The *N*-substituted mitindomide analog fetindomide (NSC 373965) has been shown (10) to hydrolyze to mitindomide, suggesting that mitindomide is the active form of fetindomide.

The bisdioxopiperazine dexrazoxane (Fig. 1), like mitindomide, is also a bis imide. We and others have shown that the bisdioxopiperazines dexrazoxane (ICRF-187; Zinecard, ADR-529) (Fig. 1), ICRF-159 (razoxane, the racemic form of dexrazoxane), and ICRF-193 (Fig. 1) are strong inhibitors of mammalian topoisomerase II (11, 12). Razoxane was developed originally as an antitumor agent (13). Dexrazoxane is, however, now clinically used for the prevention of doxorubicin-induced cardiotoxicity (14), and presumably acts through its EDTA-like hydrolysis product (15) by inhibiting iron-dependent oxygen free radical formation.

Topoisomerase II alters DNA topology by catalyzing the passing of an intact DNA double helix through a transient double-stranded break made in a second helix (16, 17). A number of antitumor drugs, including the anthracycline doxorubicin, the epipodophyllotoxins etoposide and teniposide, and amsacrine are thought to be cytotoxic by virtue of their ability to stabilize a covalent topoisomerase II-DNA intermediate (the cleavable complex) (16). However, the bisdioxopiperazines (11), like several other cytotoxic topoisomerase II inhibitors, including suramin (18), merbarone

This study was supported in part by the Medical Research Council of Canada, Grant DHP-125 from the American Cancer Society, Leukemia Society of America Translational Research Grant 6238–96, and the British Technology Group.

ABBREVIATIONS: CHO, Chinese hamster ovary; topoisomerase II, DNA topoisomerase II; p170 topoisomerase II, DNA topoisomerase II (M_r 170,000 isoform); MTT, 3-[4,5-dimethylthiazol-2-yl]-2,5-diphenyltetrazolium bromide; DZR, dexrazoxane-resistant cell line derived from the parent CHO cell line; kDNA, kinetoplast DNA; SDS, sodium dodecyl sulfate; HEPES, 4-(2-hydroxyethyl)-1-piperazineethanesulfonic acid; DMSO, dimethyl sulfoxide.

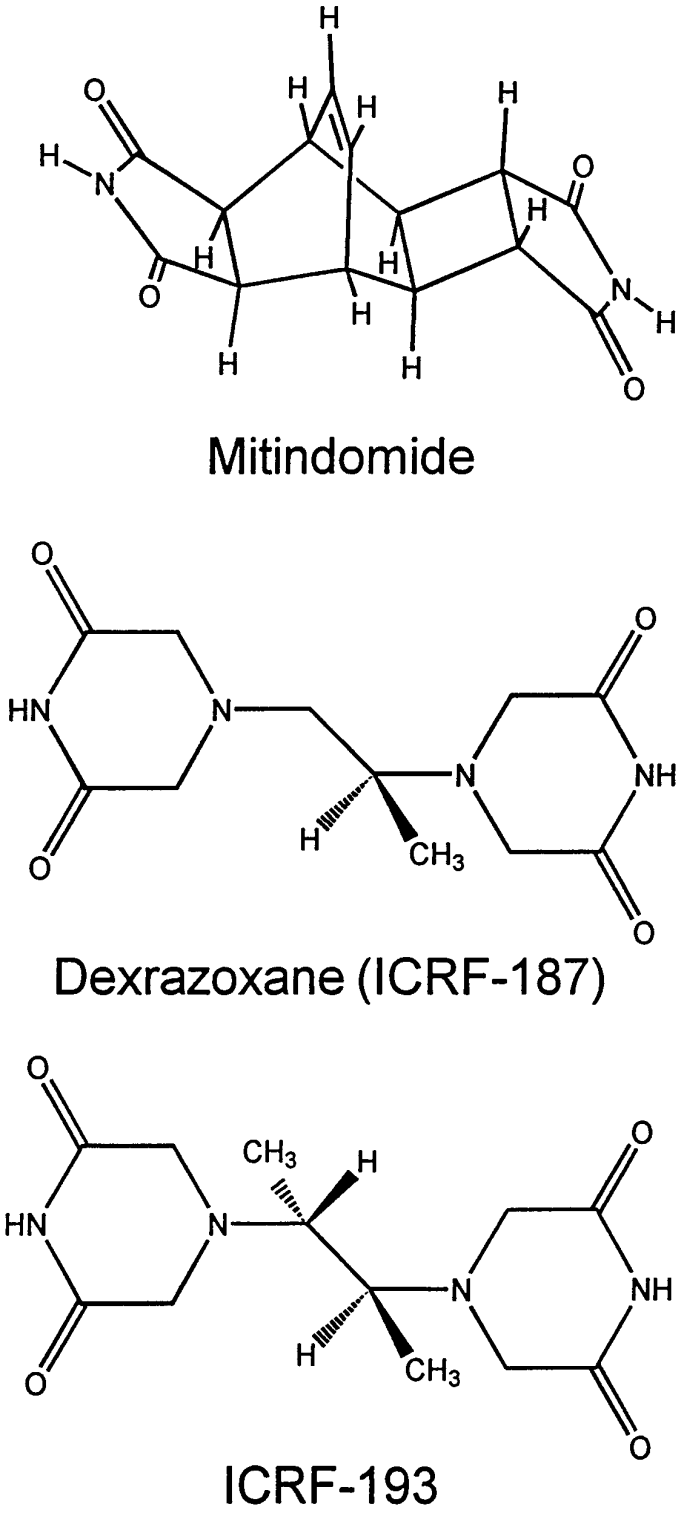

Fig. 1. Structures of mitindomide and the bisdioxopiperazines dexrazoxane (ICRF-187) and ICRF-193 (*meso* form).

(19), and the anthracycline aclarubicin (20), have been shown to inhibit topoisomerase II (11, 21) without promoting cleavable complex formation. The bisdioxopiperazines can, in fact, reduce protein-DNA cross-links induced by etoposide, amsacrine, daunorubicin, and doxorubicin (11, 21–23), as well as reducing the growth-inhibitory effects of doxorubicin and daunorubicin (22, 24). Because mitindomide has some structural features that are similar to dexrazoxane (Fig. 1), and because of the earlier demonstration of very significant cross-resistance to mitindomide by six independent cell lines with induced resistance to ICRF-159 (25, 26), a common mechanism of action seemed likely. Thus, it was decided to determine whether mitindomide also exerted its antitumor effects through the inhibition of topoisomerase II.

Materials and Methods

Drugs and chemicals. Dexrazoxane (Zinecard, ICRF-187), was a gift from Pharmacia & Upjohn (Columbus, OH). Mitindomide (NSC-284356) was obtained from the National Cancer Institute, (Bethesda, MD). Etoposide was obtained from Bristol-Myers Squibb (Wallingford, CT). kDNA and chromatographically purified, recombinant p170 human topoisomerase IIα (expressed in yeast) were obtained from Topogen (Columbus, OH). Agarose (Ultra Pure) was obtained from Gibco BRL (Burlington, Canada).

Cell culture and cytotoxicity assay. CHO cells (type AA8) were obtained from the American Type Culture Collection (Rockville, MD). The dexrazoxane-resistant DZR cells, derived from the parent CHO cells, were selected in the presence of increasing concentrations of dexrazoxane over a period of 4 months and have been described elsewhere (21). DZR cells used in the experiments reported here had not been exposed to dexrazoxane for at least several months and showed no loss in resistance. Both cell lines were grown in α-minimum essential medium (Gibco BRL) containing 20 mM HEPES (Sigma, St. Louis, MO), 100 units/ml penicillin G, 100 μg/ml streptomycin, 10% fetal bovine serum (Gibco BRL) in an atmosphere of 5% CO_2 and 95% air at 37° (pH 7.4) as described previously (12, 21). For the measurement of cell growth inhibition by MTT assay (12, 21), cells in exponential growth were harvested and seeded either at 2000 cells/well (CHO) or 5000 cells/well (DZR) in 96-well microtiter plates (100 μl/well) and allowed to attach for 24 hr. Drugs were dissolved either in α-minimum essential medium (dexrazoxane), or in either DMSO (mitindomide) or in NaOH (mitindomide, two equivalents to titrate the two imide hydrogens) with equivalent results, and were added to give a final volume of 200 μl/well. When DMSO was used, due to solubility problems, the final concentration of DMSO did not exceed 0.5% (v/v). This amount of DMSO was shown, through the use of appropriate controls, to have no significant effect on cell growth. When NaOH was used, an equivalent amount of HCl was added to ensure that the pH did not change. The cells were then allowed to grow for a further 72 hr. Typically, six replicates were measured at each drug concentration. The IC_{50} values for growth inhibition were obtained from a nonlinear least squares fit (SigmaPlot, Jandel, San Rafael CA) of the absorbance-drug concentration data to either a three- or four-parameter logistic equation as appropriate.

Topoisomerase II inhibition gel assay. The inhibition of topoisomerase II activity was measured by the ATP-dependent decatenation of kDNA (27). Reactions were carried out in 20 μl and contained 50 mM Tris·HCl, pH 8, 120 mM KCl, 10 mM $MgCl_2$, 0.5 mM ATP, 0.5 mM dithiothreitol, 30 μg/ml bovine serum albumin, 200–300 ng of kDNA, and topoisomerase II. The amount of topoisomerase II (approximately 1 unit) was adjusted in preliminary experiments to decatenate approximately 80–90% of the kDNA under our assay conditions. The reactions were incubated at 37° for 30 min and terminated by the addition of 5 μl of a stop buffer containing 5% (w/v) *N*-lauroylsarcosine, 0.125% (w/v) bromphenol blue, and 25% (v/v) glycerol. The decatenated reaction products were separated by agarose gel electrophoresis. Both the agarose gel (1% w/v) and the running buffer both contained 0.2 μg/ml of the DNA stain ethidium bromide. The gels were run at 100 V for about 40 min and after destaining were photographed by Polaroid type 667 film under UV transillumination. Authentic decatenated kDNA and linear kDNA (Topogen Inc.) were run as controls to identify decatenated kDNA. Controls were also run in the absence of ATP (for nuclease activity,

none found) and DMSO. The photographs were scanned with a Hewlett-Packard ScanJet 4P scanner (Hewlett Packard, Avondale, PA) and the 256-grey-scale digitized images were analyzed using SigmaGel (Jandel Scientific). The amount of decatenated nicked, open circular kDNA formed (identified as NOC in Fig. 2) was quantified by measuring the integrated intensity of the band. Topoisomerase II-containing nuclear extracts, used in some experiments, were prepared from CHO cells in exponential growth, as described previously (12).

Topoisomerase II-DNA covalent complexes. Topoisomerase II-DNA covalent complex formation in intact cells was measured as described previously (28). Mid-log growth CHO and DZR cells were labeled for 24 hr with 0.5 μCi/ml [*methyl*-^{3}H]thymidine (0.5 Ci/mmol) and 0.1 μCi/ml [^{14}C]leucine (318 mCi/mmol) in Dulbecco's modified Eagle medium containing 7.5% (v/v) iron-supplemented calf serum. Cells were then pelleted and resuspended in fresh Dulbecco's modified Eagle medium/7.5% calf serum and incubated for 1 hr at 37°. Cells were pelleted and resuspended in buffer, pH 7.4, containing 115 mM NaCl, 5 mM KCl, 1 mM $MgCl_2$, 5 mM NaH_2PO_4, 25 mM HEPES, and 10 mM glucose at 37° at a final cell density of 1.0×10^6 cells/ml for experimentation. Cells were then incubated with various concentrations of etoposide alone or in combination with dexrazoxane or mitindomide. Reactions were stopped by adding 1 ml of cell suspension to 10 ml of ice-cold phosphate-buffered saline. Cells were then pelleted, lysed, cellular DNA sheared, and protein-DNA complexes precipitated with SDS and KCl as described previously (28). Topoisomerase II-DNA covalent complexes were quantified by scintillation counting, and [^{3}H]DNA was normalized to cell number using the co-precipitated ^{14}C-labeled protein as an internal control.

Molecular modeling. Molecular modeling, based on the MM2 Allinger algorithm (29), was carried out with PCModel versions 4 and 5 (Serena Software, Bloomington, IN) on a PC-compatible computer with a Pentium processor.

Results

Inhibition of topoisomerase II by mitindomide and dexrazoxane. As shown by the gel decatenation results in Figs. 2 and 3 using human p170 topoisomerase II, mitindomide inhibited the topoisomerase II-catalyzed decatenation of kDNA. kDNA consists of an extensive network of many interlocked (catenated) circular DNA molecules. Topoisomerase II, which catalyzes strand-passing of double-stranded DNA, decatenates the kDNA yielding 2.5-kilobase relaxed decatenated kDNA monomers that run much faster on the gel than the catenated kDNA substrate (27). The covalently closed circular decatenated kDNA (CC in Fig. 2) is produced by the action of topoisomerase II on intact kDNA substrate. The nicked, open circular decatenated kDNA (NOC in Fig. 2) is produced by the action of topoisomerase II on nicked kDNA substrate formed during the isolation of kDNA. To determine whether there was any difference in mitindomide- or dexrazoxane-mediated inhibition of topoisomerase II from CHO cells compared with human cells, inhibition assays were also carried out on nuclear extracts obtained from CHO cells. The results shown in Table 1 indicate that the topoisomerase II in CHO nuclear extracts and purified human p170 topoisomerase II are inhibited to about the same degree. The IC_{50}-value for mitindomide is about 20 times larger than for dexrazoxane for both human topoisomerase II and CHO nuclear extract topoisomerase II.

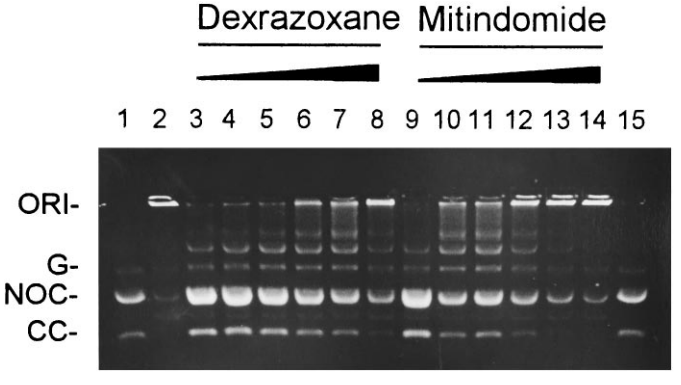

Fig. 2. Inhibition of topoisomerase II decatenation activity by dexrazoxane and mitindomide. The gel electrophoresis assay method has been described in Materials and Methods. *Lanes 3–8,* 0, 2, 5, 10, 20, and 50 μM dexrazoxane, respectively, in the assay buffer; *lanes 9–14,* 0, 50, 100, 200, 500, and 1000 μM mitindomide, respectively, in the assay buffer; *lanes 1* and *15,* decatenated kDNA controls with no topoisomerase II; *lane 2,* kDNA with no topoisomerase II in the assay buffer. *Lanes 3–14,* unlabeled slower running bands are intermediate size catenanes (dimers, trimers, and so forth) (27), where intermediate levels of decatenation occurred. *ORI*, loading well origin; *G*, genomic DNA (present as a contaminant in the kDNA preparation); *NOC*, nicked, open circular decatenated kDNA; *CC*, covalently closed circular decatenated kDNA. The assay buffer contained 1.0 unit of topoisomerase II and 200 ng of kDNA.

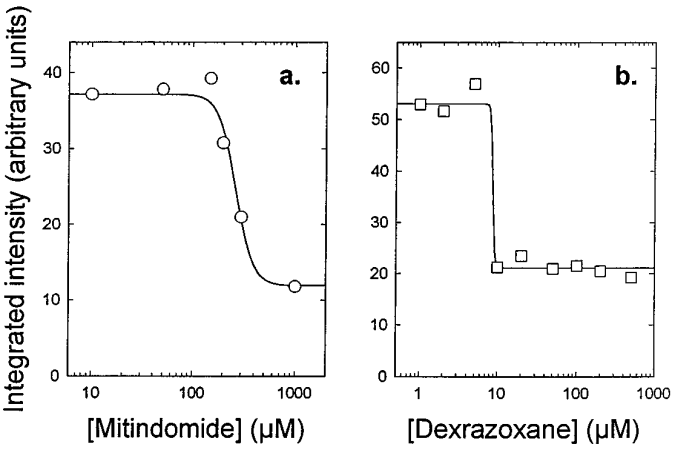

Fig. 3. Inhibition of human p170 topoisomerase II catalytic activity by mitindomide (a; ○) and dexrazoxane (b; □). Topoisomerase II decatenation activity was assayed by gel electrophoresis as described in Materials and Methods. Under the experimental conditions used, the topoisomerase II decatenated 80–90% of the kDNA. *Solid lines*, nonlinear least-squares calculated best fits of a four-parameter logistic equation to integrated intensity-concentration plots that yield IC_{50} values of 260 and 8.4 μM for mitindomide and dexrazoxane, respectively. The integrated intensity (arbitrary units) was obtained by integrating the image intensity of the decatenated nicked, open circular kDNA product (identified as *NOC* in Fig. 2) bands in the digitized photographs of the gel.

Cross-resistance of mitindomide toward dexrazoxane-resistant DZR cells. To establish whether mitindomide inhibits topoisomerase II at the same site, or by the same mechanism as dexrazoxane, the growth-inhibitory effects of mitindomide in a dexrazoxane-resistant CHO cell line (DZR) were measured. We showed previously that a number of other bisdioxopiperazines exhibited significant cross-resistance in DZR cells compared with CHO cells (21). As shown in Fig. 4 and the IC_{50} values in Table 1, mitindomide exhibited significantly less growth inhibitory effects toward DZR cells compared with the parent CHO cells. Because of the high cross-resistance of the DZR cell line toward mitindomide, it was difficult to determine accurately the IC_{50} value for mitindomide in the DZR cell line. Up to the aqueous solubil-

TABLE 1

Topoisomerase II inhibition and growth inhibition of CHO and DZR cells by mitindomide, dexrazoxane (ICRF-187), and ICRF-193

Topoisomerase II inhibition was measured with a gel assay using catenated kDNA as a substrate as described in Materials and Methods. Cell growth inhibition was measured in 96-well plates using an MTT assay after the cells had been incubated with the drug for 72 hr. Values reported are the means ± standard error; the numbers in parentheses are the number of separate determinations carried out on different days.

Drug	IC_{50}				Resistance factor
	Topoisomerase II inhibition		Cell growth inhibition		
	Human p170 topoisomerase II	CHO nuclear extract topoisomerase II	CHO	DZR	
	μM				
Mitindomide	200 ± 50 (5)	150 ± 50 (3)	69 ± 12 (5)	2,100 ± 1,000 (3)	30
Dexrazoxane	9.3 ± 2.7 (4)	6.2 ± 1.8[a]	5.8 ± 2.1 (4)	2,900 ± 190 (4)	500
ICRF-193[b]	0.6	N.D.	0.017	0.3	18

[a] The mean ± standard error here is from the nonlinear least-squares fit of the data from a single experiment to a logistic equation.
[b] Data from Refs. 12 and 21.
N.D., not determined.

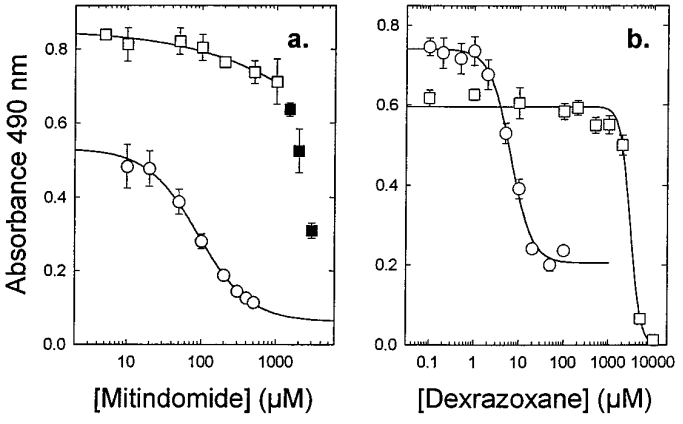

Fig. 4. a, Inhibition of growth of CHO (○) and DZR (□) cells by mitindomide. IC_{50} values of 90 ± 20 and 3900 ± 3000 μM were calculated for CHO cells and DZR cells, respectively. Mitindomide concentrations ≤1000 μM only were used in calculating the IC_{50} value, as solid mitindomide precipitated in the wells at concentrations above this. Thus, data points above 1000 μM are plotted with the symbol (■). (For comparison, the inclusion of the three data points above 1000 μM in the analysis gave an IC_{50} value of 2500 ± 140 μM.) b, Inhibition of growth of CHO (○) and DZR (□) cells by dexrazoxane. IC_{50} values of 6.4 ± 0.5 and 2900 ± 200 μM were calculated for CHO cells and DZR cells, respectively. The cells were incubated with drug for 72 hr and then assayed with MTT. The errors quoted for the IC_{50} values are SEMs obtained from nonlinear least squares fits of a four-parameter logistic equation of the absorbance-concentration data. *Error bars*, standard deviations for replicates from six wells.

ity limit of mitindomide (≤1000 μM), only a maximum of 15% growth inhibition of the DZR cells was seen (Fig. 4). Thus, the resistance factor for mitindomide of at least 30 is comparable to that for ICRF-193 (Table 1) of 18, and other bisdioxopiperazines (21). These results suggest strongly that mitindomide binds to the same site on topoisomerase II as do the bisdioxopiperazines.

Lack of covalent cleavable complex formation by mitindomide. A number of topoisomerase II poisons, including the anthracycline doxorubicin, the epipodophyllotoxins etoposide and teniposide, and amsacrine, are thought to be cytotoxic through their ability to stabilize a covalent topoisomerase II-DNA intermediate (the cleavable complex) (16). The bisdioxopiperazines, however, are catalytic or noncleavable complex forming inhibitors (11) that inhibit topoisomerase II without promoting cleavable complex formation. Thus, cleavable complex formation was measured in CHO cells to determine whether or not mitindomide promoted cleavable complex formation. Cleavable complex formation in both CHO and DZR cells are compared in the presence of mitindomide (0–200 μM) and 50 μM etoposide in Fig. 5 and in Fig. 6, b and c. Paired Student's t tests, carried out on the data of Fig. 6, b and c, at 200 μM mitindomide compared with DMSO controls, showed that the amount of cleavable complex formation was not significantly increased ($p = 0.076$ and 0.096 for CHO and DZR cells, respectively; $n = 4$) for either cell type. In contrast, etoposide-induced covalent complexes were evident in CHO cells, but reduced in DZR cells, as we have demonstrated previously (21). The reduction in etoposide-induced covalent complexes in DZR cells compared with CHO

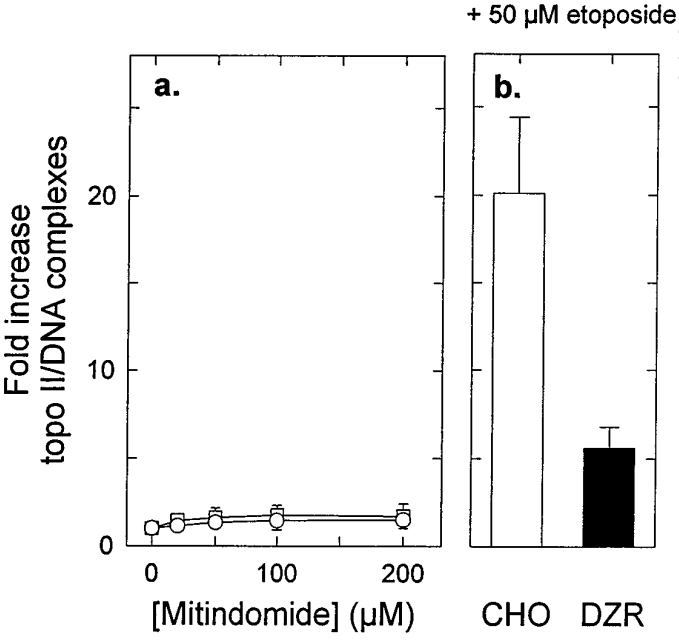

Fig. 5. a, Formation of topoisomerase II-DNA covalent complexes in CHO (○) and DZR (□) cells after a 40-min incubation with increasing concentrations of mitindomide. b, The formation of topoisomerase II-DNA covalent complexes produced by incubating cells for 30 min with 50 μM etoposide are included for comparison. Cells were prelabeled with [*methyl*-^{3}H]thymidine and [^{14}C]leucine for 18–24 hr. KCl-SDS-precipitable complexes were isolated, and the ^{3}H counts were normalized using ^{14}C as an internal standard for cell number as described in Materials and Methods. Results are expressed as fold-increase in topoisomerase II-DNA complexes relative to complexes isolated from cells incubated in the absence of drug.

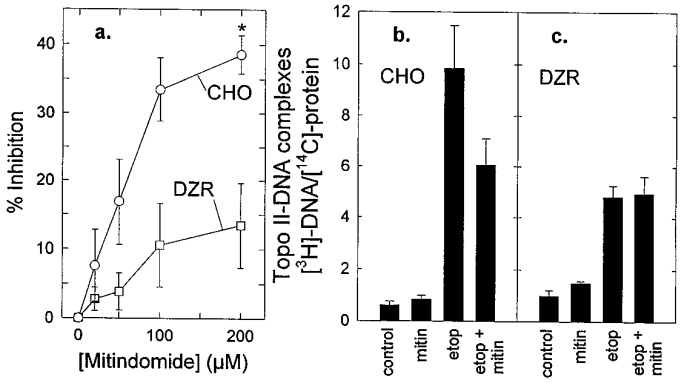

Fig. 6. Inhibitory effects of preincubation of increasing concentrations of mitindomide on etoposide-induced cleavable complex formation in (a) CHO (○) and DZR (□) cells. Inhibitory effect of preincubation of 200 μM mitindomide on etoposide-induced topoisomerase II-DNA covalent complex formation in (b) CHO and (c) DZR cells. Cells were prelabeled with [*methyl*-^{3}H]thymidine and [^{14}C]leucine for 18–24 hr. KCl-SDS-precipitable complexes were isolated, and the ^{3}H counts were normalized using ^{14}C as an internal standard for cell number as described in Materials and Methods. Bars represent the mean ± standard error. The cells were preincubated for 10 min with mitindomide (0 or 200 μM) and then incubated with etoposide (0 or 50 μM) for a further 30 min. The inhibitory effects of mitindomide were calculated subsequent to subtracting the DMSO and mitindomide control values from the values for etoposide-induced and mitindomide plus etoposide-induced topoisomerase II-DNA complexes, respectively. *, Averaging the results from three experiments for CHO cells and four experiments for DZR cells, showed that mitindomide is significantly inhibitory for CHO cells ($p = 0.024$), but not for DZR cells ($p = 0.27$) by paired Student's *t* test.

cells correlates with a decrease in the protein level of DZR cell topoisomerase II to one-half of that found in CHO cells, as we have demonstrated (21).

Inhibition of etoposide-induced topoisomerase II-DNA covalent complexes by mitindomide. We showed previously that dexrazoxane was able to significantly inhibit etoposide-induced cleavable complex formation in CHO cells (21). We also showed that dexrazoxane was effective in inhibiting etoposide-induced cleavable complex formation in K562 and etoposide-resistant K/VP.5 cells (23). The bisdioxopiperazine ICRF-193 has also been shown to reduce etoposide-induced cleavable complex formation (30). Thus, if mitindomide acts like the bisdioxopiperazines, it should also be able to reduce etoposide-induced cleavable complex formation. As shown in Fig. 6a, mitindomide inhibits etoposide-induced cleavable complex formation in a concentration-dependent manner in CHO cells. The results of Fig. 6a show that 200 μM mitindomide significantly ($p = 0.024$, $n = 3$) decreases etoposide-induced cleavable complex formation in CHO cells, but not in DZR cells ($p = 0.27$, $n = 4$). This attenuated inhibition of etoposide-induced cleavable complex formation in DZR cells, compared with CHO cells, was also seen previously with dexrazoxane (21). Thus, mitindomide acts similarly to dexrazoxane, not only in its ability to inhibit etoposide-induced cleavable complex formation, but also because it has a decreased ability to inhibit etoposide-induced cleavable complex formation in DZR cells compared with CHO cells. These results also suggest strongly that mitindomide acts on the same site on topoisomerase II, and by the same mechanism as dexrazoxane.

Molecular modeling of mitindomide and dexrazoxane. Because mitindomide and dexrazoxane are both bis imides with some structural similarities, the structures of the two compounds were compared using molecular modeling to determine what structural features the two drugs have in common that are essential for their topoisomerase II-inhibitory activity. The modeling of these compounds was aided by the x-ray crystal structures of dexrazoxane (31), an *N*-substituted analog of mitindomide (32), and of a one-ring-opened mitindomide derivative (33). Molecular mechanics minimization of a mitindomide structure obtained from the x-ray structure of the N-substituted analog of mitindomide (32) gave a structure very close (root mean square deviation for all common heteroatoms and hydrogens was 0.09 Å) to the *N*-substituted mitindomide. Thus, parameters derived from the mitindomide structure obtained from molecular modeling can be used with confidence. The structure shown for dexrazoxane was, likewise, obtained from the x-ray crystal structure of dexrazoxane (31). Dexrazoxane is a conformationally flexible molecule compared with the structurally rigid mitindomide. In the crystal, dexrazoxane is H-bonded through the imide hydrogen atom and one carbonyl oxygen atom to an adjacent dexrazoxane molecule in a head-to-tail arrangement (31). The conformation of dexrazoxane in the crystal is very close to the energetically most stable structure, as the rotational energy plots (data not shown) for rotation about either the nitrogen-main chain carbon atom or the two main chain carbon atoms were at a minima for the structure shown in Fig. 7. Data for the dexrazoxane analog ICRF-193 (Fig. 1), which is the most potent known bisdioxopiperazine topoisomerase II inhibitor (12), are also included in Table 2 for comparison. The structure of mitindomide and dexrazoxane are compared in Fig. 7. It can be seen from Fig. 7 and the data of Table 2 that both structures have a number of common structural features. The most striking feature in common is the coplanarity (7.3 and 1.3° on mitindomide and dexrazoxane, respectively) of the two imide-containing rings on each of these molecules. Also the imide nitrogen-to-imide nitrogen bond distance in mitindomide is only slightly shorter (7.8 compared with 9.0 Å) than in dexrazoxane. Although there is a high degree of coplanarity in each molecule, the two planes are offset from each other in each molecule. This offset, measured from the distance the nitrogen of the distal imide ring in each molecule lies above the plane formed by the first imide ring, is very similar (3.0 and 3.7 Å for mitindomide and dexrazoxane, respectively). The molecular volumes and the total surface areas of dexrazoxane and ICRF-193 are only slightly larger than for mitindomide (Table 2). Similarly, the van der Waals polar surface area of each of these molecules is also very close (Table 2).

Discussion

The growth-inhibitory effect of mitindomide with an IC_{50} value of 69 μM toward CHO cells determined in this study (Table 1) compares with an IC_{50} value of 16 μM for a different CHO cell line (25), and 73 μM for L1210 leukemia cells (6). We have shown, using a kDNA decatenation assay (Fig. 2), that mitindomide inhibits the catalytic activity of topoisomerase II. We further showed that mitindomide inhibits topoisomerase II without increasing topoisomerase II-DNA covalent cleavable complex formation (Figs. 5 and 6b). This latter result establishes that mitindomide is a catalytic (or non-cleavable complex-forming) type of topoisomerase II inhibitor. Other known catalytic inhibitors include the bisdiox-

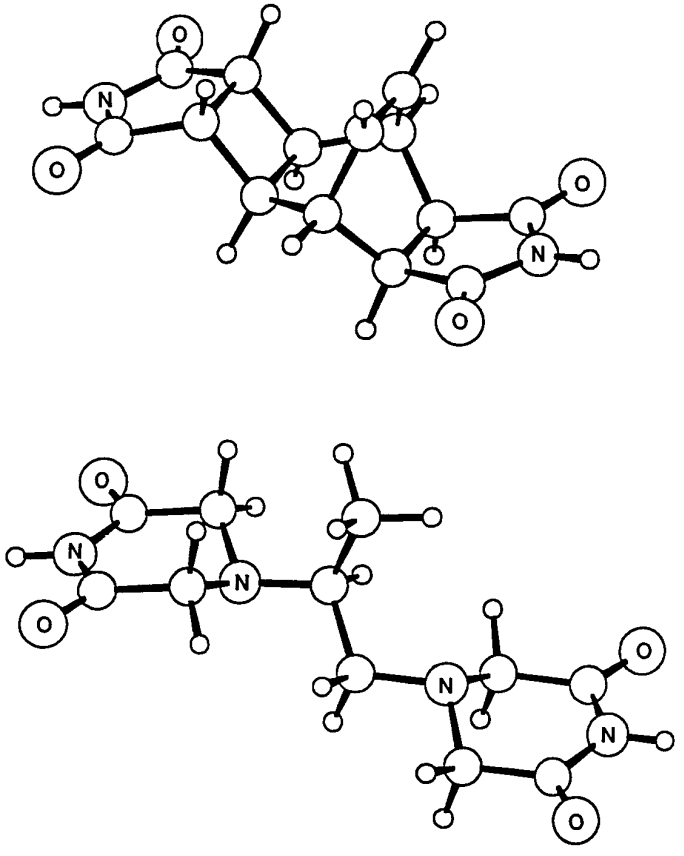

Fig. 7. Ball and stick structures of mitindomide (*top*) and dexrazoxane (*bottom*) are compared. The structure of mitindomide was obtained from molecular modeling using the x-ray crystal structure of an *N*-substituted mitindomide analog (32) and dexrazoxane (31) as starting points. Both molecules have imide rings that are nearly coplanar and similar imide nitrogen-to-imide nitrogen distances (7.8 and 9.0 Å for mitindomide and dexrazoxane, respectively). Only the heteroatoms are labeled.

TABLE 2

Comparison of the structural parameters of mitindomide and the bisdioxopiperazines dexrazoxane (ICRF-187) and ICRF-193

The molecular parameters were derived from molecular modeling and X-ray structures of dexrazoxane and an analog of mitindomide. Imide *N*-to-imide *N* distance, coplanarity of imide rings, and *N*-to-plane distance were derived from X-ray crystal structures from an *N*-substituted derivative of mitindomide (32) and dexrazoxane (31) and molecular modeling for ICRF-193. The imide ring plane was defined by the nitrogen imide atom and the two adjacent carbonyl carbon atoms. The coplanarity was measured by calculating the angle of the normals of the two planes to each other. Area and volume were calculated from the van der Waals surfaces by molecular modeling. Nonpolar surface area includes contributions from both unsaturated (mitindomide only) and saturated areas.

Parameter	Mitindomide	Dexrazoxane	ICRF-193
Imide *N*-to-imide *N* distance (Å)	7.8	9.0	9.2
Coplanarity of imide rings (°)	7.3	1.3	2.9
N-to-plane distance (Å)	3.0	3.7	2.8
Nonpolar surface area (Å^2)	127	135	153
Polar surface area (Å^2)	135	141	144
Total surface area (Å^2)	262	276	297
Molecular volume (Å^3)	326	351	374
Human p170 topoisomerase II inhibition, IC_{50} (μM)	200	9.3	0.6[a]

[a] From Ref. 12.

opiperazines (11, 12, 21), suramin (18), merbarone (19), and aclarubicin (20). Mitindomide also showed significant cross-resistance (Fig. 4 and Table 1) to the dexrazoxane-resistant DZR cell line. This cell line has been shown to have high cross-resistance to a number of other bisdioxopiperazines, but not to the other catalytic topoisomerase II inhibitors suramin, merbarone, or aclarubicin, suggesting that the topoisomerase II has acquired point mutations that change critical regions of the enzyme required for bisdioxopiperazine binding or activity (21). Thus, mitindomide cross-resistance in the DZR cell suggests that mitindomide binds at the same site as dexrazoxane and the other bisdioxopiperazines. We also showed that mitindomide was able to effectively reduce etoposide-induced cleavable complex formation (Fig. 6b) in a manner similar to dexrazoxane (21). The attenuated inhibition of etoposide-induced cleavable complex formation shown for DZR compared with CHO cells (Fig. 6, b and c) closely parallels that exhibited by dexrazoxane (21). Thus, both these results further suggest that mitindomide acts at the same site on topoisomerase II as dexrazoxane. Also consistent with our results, mitindomide has also been shown to be at least 18-fold cross-resistant (25, 26) to another bisdioxopiperazine (ICRF-159)-resistant CHO cell line (34).

Mitindomide is conformationally a very rigid structure, unlike dexrazoxane, which can potentially adopt a large number of conformations through rotation about the two nitrogen-carbon bonds and the two carbon-carbon bonds. The two imide rings of mitindomide are highly coplanar (Table 2 and Fig. 7). The x-ray crystal structure of dexrazoxane (31) shows that in the crystal, dexrazoxane, adopts an extended conformation (Fig. 7) with a high degree of coplanarity between the imide rings. This conformation closely resembles that of mitindomide (Fig. 7) with imide nitrogen-to-imide nitrogen distances and other molecular parameters being quite similar to that for dexrazoxane and ICRF-193 (Table 2). These results suggest that dexrazoxane interacts with topoisomerase II in its extended conformation with its imide rings coplanar. Because mitindomide does not have nitrogen atoms in the central part of the molecule like dexrazoxane, we would also like to suggest that there is no absolute requirement for non-imide nitrogens of the piperazine groups in dexrazoxane for binding to topoisomerase II. A number of mitindomide analogs were tested for activity in an *in vivo* P-388 leukemia screen (3) and were used to define the structural features that are required for activity. Imides with shorter imide nitrogen-to-imide nitrogen bond distances than mitindomide were found to be inactive (3). We also showed previously (12) that ICRF-161, which has a 3 carbon linear alkane central chain, was both much less growth inhibitory toward CHO cells and a weaker inhibitor of topoisomerase II. In the extended conformation ICRF-161 would be expected to have an imide nitrogen-to-imide nitrogen bond distance larger than that of dexrazoxane. Thus, an imide nitrogen-to-imide nitrogen bond distance of about 9 Å, which is between that seen for mitindomide and ICRF-161, may be about optimal for the inhibition of topoisomerase II. The dihydro analog of mitindomide was also active (3), indicating the lack of a requirement for the double bond in mitindomide. Although the molecular modeling studies show the strong structural similarities that exist between mitindomide and dexrazoxane, suggesting that mitindomide is a bisdioxopiperazine type topoisomerase II inhibitor, the conclusion that mitindomide inhibits topoisomerase II at the bisdioxopiperazine binding site is based mainly on our biochemical and pharmacological studies.

It has been proposed that dexrazoxane and the other bisdioxopiperazines interact with topoisomerase II without forming topoisomerase II-DNA cleavable complexes (11). It has been shown that in the presence of ATP, ICRF-193 (Fig. 1) converts topoisomerase II to a form incapable of binding circular DNA (35). These results were interpreted in terms of an ATP-modulated protein-clamp model (17, 36) in which ICRF-193 binds to the closed clamp form of the enzyme and prevents its conversion to the DNA-binding open-clamp form. If mitindomide is acting at the same site as the other bisdioxopiperazines, it too, would be capable of preventing the opening of the closed clamp form of the enzyme.

Our finding that mitindomide is a catalytic inhibitor of topoisomerase II may lead to the rational development of more efficacious mitindomide analogs. Mitindomide is also likely to find use as a probe of mechanism of topoisomerase II activity and the action of a number of important topoisomerase II-directed anticancer drugs. Because mitindomide does not yield an EDTA-type structure like dexrazoxane (15), the metal chelating effects and topoisomerase II inhibitory effects on cell growth of these two drugs may be separated.

References

1. Narayanan, V. L. Strategy for the discovery and development of novel anticancer agents, in *Structure-Activity Relationships of Anti-Tumour Agents* (D. N. Reinhoudt, T. A. Connors, H. M. Pinedo, and L. W. van de Poll, eds.). Martinus Nijhoff, The Hague, 5–22 (1983).
2. Neighbors, R. P., and J. R. Riden, inventors. Chevron Research, assignee. Use of a tricyclodecene-3,4,7,8-tetracarboxylic acid diimide as an antimurine tumor agent. U.S. Patent 4,877,806 (1989).
3. Deutsch, H. M., L. T. Gelbaum, M. McLaughlin, T. J. Fleischmann, L. L. Earnhart, R. D. Haugwitz, and L. H. Zalkow. Synthesis of congeners and prodrugs of the benzene maleimide photoadduct, mitindomide, as potential antitumor agents. *J. Med. Chem.* **29:**2164–2170 (1986).
4. Moore, D. J., G. Powis, D. C. Melder, H. M. Deutsch, and L. H. Zalkow. Cross-linking of DNA by diimide antitumor agents and the relationship to cytotoxicity in A204 rhabdomyosarcoma cells. *J. Cell. Pharmacol.* **1:**103–108 (1990).
5. Vishnuvajjala, B. R., and J. C. Cradock. Tricyclo[4.2.2.0^{2,5}]dec-9-ene-3,4,7,8-tetracarboxylic acid diimide: formulation and stability studies. *J. Pharm. Sci.* **75:**301–303 (1986).
6. Sampedro, F., J. Partika, P. Santalo, A. M. Molins-Pujol, J. Bonal, and R. J. Perez-Soler. Liposomes as carriers of different new lipophilic antitumor drugs: a preliminary report. *J. Microencapsul.* **11:**309–318 (1994).
7. Zhubanov, B. A., G. I. Boiko, K. A. Abdulin, M. B. Umerzakova, and Z. K. Ibraeva. Tricyclodecenetetracarboxydiimides, and their antitumor activity. *Khim.-Farm. Zh.* **25:**43–44 (1991).
8. Haugwitz, R. D., V. Narayanan, L. H. Zalkow, H. M. Deutch, and L. Gelbaum, inventors. United States of America, assignee. Substituted *N*-methyl derivatives of mitindomide. U.S. Patent 4,803,202 (1984).
9. Haugwitz, R. D., V. L. Narayanan, L. H. Zalkow, and H. M. Deutsch. Formaldehyde derivatives of mitindomide. United States of America, assignee. U.S. Patent 4,670,461 (1987).
10. Umprayn, K., V. J. Stella, and C. M. Riley. Stability indicating assay for fetindomide (NSC 373965), a potential prodrug of mitindomide (NSC 284356), employing high-performance liquid chromatography. *J. Pharm. Biomed. Anal.* **5:**675–685 (1987).
11. Ishida, R., T. Miki, T. Narita, R. Yui, M. Sato, K. R. Utsumi, K. Tanabe, and T. Andoh. Inhibition of intracellular topoisomerase II by antitumor bis(2,6-dioxopiperazine) derivatives: mode of cell growth inhibition distinct from that of cleavable complex-forming type inhibitors. *Cancer Res.* **51:**4909–4916 (1991).
12. Hasinoff, B. B., T. I. Kuschak, J. C. Yalowich, and A. M. Creighton. A QSAR study comparing the cytotoxicity and DNA topoisomerase II inhibitory effects of bisdioxopiperazine analogs of ICRF-187 (dexrazoxane). *Biochem. Pharmacol.* **50:**953–958 (1995).
13. Creighton, A. M., K. Hellmann, and S. Whitecross. Antitumour activity in a series of bisdiketopiperazines. *Nature (Lond.)* **22:**384–385 (1969).
14. Speyer, J. L., M. D. Green, A. Zeleniuch-Jacquotte, J. C. Wernz, M. Rey, J. Sanger, E. Kramer, V. Ferrans, H. Hochster, M. Meyers, R. H. Blum, F. Feit, M. Attubato, W. Burrows, and F. M. Muggia. ICRF-187 permits longer treatment with doxorubicin in women with breast cancer. *J. Clin. Oncol.* **10:**117–127 (1992).
15. Buss, J. L., and B. B. Hasinoff. The one-ring open hydrolysis product intermediates of the cardioprotective agent ICRF-187 (dexrazoxane) displace iron from iron-anthracycline complexes. *Agents Actions* **40:**86–95 (1993).
16. Corbett, A. H., and N. Osheroff. When good enzymes go bad: conversion of topoisomerase II to a cellular toxin by antineoplastic drugs. *Chem. Res. Toxicol.* **6:**585–597 (1993).
17. Berger, J. M., S. J. Gamblin, S. C. Harrison, and J. C. Wang. Structure and mechanism of DNA topoisomerase II. *Nature (Lond.)* **379:**225–232 (1996).
18. Bojanowski, K., S. Lelievre, J. Markovits, J. Couprie, A. Jacquemin-Sablon, and A. K. Larsen. Suramin is an inhibitor of DNA topoisomerase II *in vitro* and in Chinese hamster fibrosarcoma cells. *Proc. Natl. Acad. Sci. USA* **89:**3025–3029 (1992).
19. Drake, F. H., G. A. Hofman, S. M. Mong, J. O. Bartus, R. P. Hertzberg, R. K. Johnson, M. R. Mattern, and C. K. Mirabelli. *In vitro* and intracellular inhibition of topoisomerase II by the antitumor agent merbarone. *Cancer Res.* **49:**2578–2583 (1989).
20. Jensen, P. B., P. S. Jensen, E. J. F. Demant, E. Friche, B. S. Sorensen, M. Sehested, K. Wassermann, L. Vindelov, O. Westergaard, and H. H. Hansen. Antagonistic effect of aclarubicin on daunorubicin-induced cytotoxicity in human small cell lung cancer cells: relationship to DNA integrity and topoisomerase II. *Cancer Res.* **51:**5093–5099 (1991).
21. Hasinoff, B. B., T. I. Kuschak, A. M. Creighton, C. L. Fattman, W. P. Allan, P. Thampatty, and J. C. Yalowich. Characterization of a Chinese hamster ovary cell line with acquired resistance to the bisdioxopiperazine dexrazoxane (ICRF-187) catalytic inhibitor of topoisomerase II. *Biochem. Pharmacol.* **53:**1843–1853 (1997).
22. Sehested, M., P. B. Jensen, B. S. Sorensen, B. Holm, E. Friche, and E. J. F. Demant. Antagonistic effect of the cardioprotector (+)-1,2-bis(3,5-dioxopiperazinyl-1-yl)propane (ICRF-187) on DNA breaks and cytotoxicity induced by the topoisomerase II directed drugs daunorubicin and etoposide (VP-16). *Biochem. Pharmacol.* **46:**389–393 (1993).
23. Fattman, C., W. P. Allan, B. B. Hasinoff, and J. C. Yalowich. Collateral sensitivity to the bisdioxopiperazine dexrazoxane (ICRF-187) in etoposide (VP-16) resistant human leukemia K562 cells. *Biochem. Pharmacol.* **52:**635–642 (1996).
24. Hasinoff, B. B., J. C. Yalowich, Y. Ling, and J. L. Buss. The effect of dexrazoxane (ICRF-187) on doxorubicin and daunorubicin-mediated growth inhibition of Chinese hamster ovary (CHO) cells. *Anticancer Drugs* **7:**558–567 (1996).
25. Kenwrick, S. J. Studies on the mechanism of induced resistance to antitumour agent ICRF 159 in mammalian cell lines. Ph.D. thesis. University of London, London (1984).
26. Creighton, A. M., J. Long, and S. J. Kenwrick. A comparative study of the properties of the tumour-inhibitory photosynthetic benzene-maleimide adduct (NSC 284, 356 and ICRF 159). *Imperial Cancer Res. Fund Sci. Report—1983.* 143–144 (1984).
27. Sahai, B. M., and J. G. Kaplan. A quantitative decatenation assay for type II topoisomerases. *Anal. Biochem.* **156:**364–379 (1986).
28. Ritke, M. K., D. Roberts, W. P. Allan, J. Raymond, V. V. Bergoltz, and J. C. Yalowich. Altered stability of etoposide-induced topoisomerase II-DNA complexes in resistant human leukemia K562 cells. *Br. J. Cancer* **69:**687–697 (1994).
29. Burkert, U., and N. L. Allinger. *Molecular Mechanics. ACS Monograph 177.* American Chemical Society, Washington, D. C. (1982).
30. Clarke, D. J., R. T. Johnson, and C. S. Downes. Topoisomerase II inhibition prevents anaphase chromatid segregation in mammalian cells independently of the generation of DNA strand breaks. *J. Cell Sci.* **105:**563–569 (1993).
31. Hempel, A., N. Camerman, and A. Camerman. Stereochemistry of the antitumor agent 4,4′-(1,2-propanediyl)bis(4-piperazine-2,6-dione): crystal and molecular structures of the racemate (ICRF-159) and a soluble enantiomer (ICRF-187). *J. Am. Chem. Soc.* **105:**3453–3456 (1982).
32. Deutsch, H. M., L. McGowan, D. G. Van Derveer, L. T. Gelbaum, and L. H. Zalkow. Structure of a derivative of mitindomide, the maleimide-benzene photoadduct, $C_{20}H_{20}N_2O_8$. *Acta Crystallogr. Sect. C* **40:**1925–1927 (1984).
33. Pettit, G. R., K. D. Paull, C. L. Herald, D. L. Herald, and J. R. Riden. Antineoplastic agents. 90. The structure of the benzene-maleimide photosynthetic product (mitindomide). *Can. J. Chem.* **61:**2291–2294 (1983).
34. Kenwrick, S. J., and A. M. Creighton. Isolation and characterization of a subline of CHO cells with induced resistance to ICRF 159. *Br. J. Cancer* **46:**504–505 (1982).
35. Roca, J., R. Ishida, J. M. Berger, T. Andoh, and J. C. Wang. Antitumor bisdioxopiperazines inhibit yeast DNA topoisomerase II by trapping the enzyme in the form of a closed protein clamp. *Proc. Natl. Acad. Sci. USA* **91:**1781–1785 (1994).
36. Roca, J., and J. C. Wang. The capture of a DNA double helix by an ATP-dependent protein clamp: a key step in DNA transport by type II DNA topoisomerases. *Cell* **71:**833–840 (1992).

Send reprint requests to: Dr. Brian B. Hasinoff, Faculty of Pharmacy, University of Manitoba, Winnipeg, Manitoba, Canada R3T 2N2. E-mail: b_hasinoff@umanitoba.ca

or

Dr. Jack C. Yalowich, University of Pittsburgh, School of Medicine, W 1308 Biomedical Science Tower, Pittsburgh, PA 15261. E-mail: yalowich@server.pharm.pitt.edu